

# Frequency stabilization of a laser diode with use of light-induced birefringence in an atomic vapor

Yutaka Yoshikawa, Takeshi Umeki, Takuro Mukae, Yoshio Torii, and Takahiro Kuga

We present a simple modulation-free technique to stabilize a laser frequency to the Doppler-free spectra of an atomic vapor. Polarization spectroscopy with use of a balanced polarimeter allows us to obtain a background-free dispersion signal suitable for high-speed and robust frequency stabilization. We employed the method to the  $5S_{1/2} F = 2 \rightarrow 5P_{3/2} F' = 3$  transition of  $^{87}\text{Rb}$  atoms. The achieved feedback bandwidth was approximately 100 kHz, and an efficient suppression of the frequency noise in a laboratory environment was attained. © 2003 Optical Society of America

OCIS codes: 140.0140, 300.6260, 000.2170.

## 1. Introduction

Stabilization of laser frequency is essential for various researches, from fundamental to practical applications, in the fields of metrology, frequency standards, and optical communications. A dispersionlike signal at the resonance frequency is often required to lock the laser frequency to the center of the atomic spectra with electronic servo controls. The most popular way to obtain this signal is through phase-sensitive detection with frequency modulation spectroscopy,<sup>1-4</sup> by which the first derivative of absorption profiles can be obtained. This enables us to easily achieve a high signal-to-noise (S/N) ratio. However, the bandwidth of the feedback is intrinsically limited by the modulation frequency and the time constant of a lock-in amplifier. Because high-speed modulators and lock-in amplifiers are expensive, the overall apparatus for high-performance frequency stabilization tends to be costly.

Alternatively, modulation-free electronic frequency stabilization has been demonstrated by two kinds of techniques. One is based on the Zeeman shift-induced or two-color light-induced dichroism of the atomic transition,<sup>5-7</sup> which relies on the difference of two absorption signals with slightly different centers to obtain a dispersionlike signal at the reso-

nance frequency. The other technique employs a dispersion signal obtained by polarization spectroscopy.<sup>8</sup> It is one of the Doppler-free spectroscopic techniques and can directly detect the atomic dispersion referred to as Doppler-free light-induced birefringence (DLIB). Over the years, this method has been applied to stabilize dye lasers<sup>9</sup> and laser diodes.<sup>10</sup> However, in the basic scheme in which a probe beam is detected through a sample placed between two nearly crossed polarizers, residual background light cannot be eliminated, and its amplitude noise degrades the S/N ratio.<sup>11</sup> Alternatively, a slightly modified scheme using balanced detection between two orthogonal polarization components of the probe beam was reported to observe background-free DLIB spectra with a highly improved S/N ratio.<sup>12</sup> However, to our knowledge, there has been no experimental report on frequency stabilization of a laser diode with this scheme.

Another advantage of the modulation-free methods is that the achievable feedback bandwidth is limited, in principle, only by the atomic-frequency response approximately equal to the natural linewidth of the transition  $\Gamma$ . For the  $D_1$  and  $D_2$  transitions of the alkali metal atoms,  $\Gamma$  is on the order of several megahertz, which is enough for high-speed frequency stabilization to suppress the frequency noise in a typical experimental environment, such as an acoustic noise and low-frequency  $1/f$  (flicker) noise of the laser diode.<sup>13</sup>

In this paper, we demonstrate polarization spectroscopy using a balanced polarimeter consisting of a polarization beam splitter (PBS) and a balanced detector for the  $5S_{1/2} F = 2 \rightarrow 5P_{3/2} F' = 1, 2,$  and  $3$  transitions of  $^{87}\text{Rb}$  atoms. The obtained signal can

The authors are with the Institute of Physics, University of Tokyo, 3-8-1 Komaba, Meguro-ku, Tokyo 153-8902, Japan. Y. Yoshikawa's e-mail address is yutaka@phys.c.u-tokyo.ac.jp.

Received 9 April 2003; revised manuscript received 12 August 2003.

0003-6935/03/336645-05\$15.00/0

© 2003 Optical Society of America

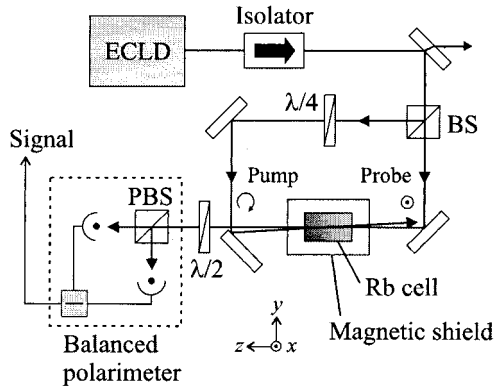


Fig. 1. Schematic diagram of the experimental setup. ECLD, external cavity laser diode; BS, beam splitter;  $\lambda/4$ , quarter-wave plate;  $\lambda/2$ , half-wave plate; and PBS, polarization beam splitter.

be readily exploited as an error signal for robust and high-speed laser diode-frequency stabilization. The apparatus does not require any modulation devices or lock-in amplifiers to achieve high-performance frequency stabilization comparable with that with frequency modulation spectroscopy. These capabilities are suited for a wide range of applications, from high-precision spectroscopy to laser cooling experiments.

## 2. Light-Induced Birefringence Signal

Let us first briefly summarize the principles of polarization spectroscopy and quantitatively calculate the signal profile of the DLIB. The model we will treat here is based on the experimental setup schematically shown in Fig. 1. Let us consider a linearly  $x$ -polarized probe beam propagating along the  $z$  direction  $\hat{\mathbf{x}}E_0 \cos(\omega t - k_0 z)$  passing through the atomic sample of length  $L$ . Here,  $\hat{\mathbf{x}}$  is a unit vector along the  $x$  direction,  $\omega$  is the laser frequency, and  $k_0$  is the wave number of the probe beam in a vacuum. The sample is simultaneously pumped by a counterpropagating, circularly polarized pump beam. Provided that the pump beam sufficiently polarizes the atomic sample, the absorption coefficient,  $\alpha_+$  and  $\alpha_-$ , and the refractive index,  $n_+$  and  $n_-$ , for left-hand ( $\sigma^+$ ) and right-hand ( $\sigma^-$ ) circularly polarized components of the probe beam are no longer the same. The difference  $\Delta\alpha = \alpha_+ - \alpha_-$  represents the circular dichroism, making the polarization of the probe beam elliptical, whereas the difference  $\Delta n = n_+ - n_-$  describes the optical birefringence that induces the rotation of the axis of polarization by  $\Delta\theta = \Delta n k_0 L/2$ .<sup>14</sup> Here we suppose that the transition frequency of the  $\sigma^+$  and  $\sigma^-$  transitions are the same. Since the frequency dependence of  $n_+$  and  $n_-$  are dispersive with the same center,  $\Delta\theta$ , which is proportional to their difference, also leads to a dispersion signal. Therefore, if one can measure it, the steep slope around the resonance frequency can be directly exploited for frequency stabilization.<sup>9–11</sup>

The conventional way to measure the polarization state after passing through the sample is to put a polarizer in front of a detector. This scheme corre-

sponds to an experimental setup in which the half-wave plate in Fig. 1 is replaced by a polarizer, and the transmitted intensity is measured with a single detector instead of the balanced polarimeter. Here we assume that the transmission axis of the polarizer is tilted at an angle of  $\phi$  with respect to the  $y$  axis. For most practical cases, the quantities  $\Delta\theta$  and  $\Delta\alpha L$  are very small. The transmitted intensity from the polarizer  $I_t$  is then given up to the second order in  $\Delta\theta$  and  $\Delta\alpha L$  as

$$I_t(\phi) = I_0 \exp(-\bar{\alpha}L) \left\{ \sin^2 \phi + \Delta\theta \sin 2\phi + \left[ \Delta\theta^2 + \left( \frac{\Delta\alpha L}{4} \right)^2 \right] \cos^2 \phi \right\}, \quad (1)$$

where  $I_0 = \epsilon_0 c |E_0|^2/2$ , with  $\epsilon_0$  and  $c$  being the permittivity and the speed of light in vacuum, respectively,  $\bar{\alpha} = (\alpha_+ + \alpha_-)/2$ , and the factor  $I_0 \exp(-\bar{\alpha}L)$  represents a saturated-absorption spectrum. Here we assume that the polarizer has an ideal performance, i.e., its extinction ratio is infinity. The situation of  $\phi = 0$  promises a complete background-free measurement. However, the signal is a second-order contribution of  $\Delta\theta$  and  $\Delta\alpha L$  and is not the dispersion shape. Since the second term in the braces is a required signal, the polarizer must be tilted slightly so that the second term becomes much larger than the third term. At the same time, however, increasing  $\phi$  gives rise to an undesirable offset represented in the first term. Because this offset is subject to the amplitude noise of the probe beam,<sup>8,11</sup> one has to find the optimized angle  $\phi_o$  in order to achieve the dispersionlike signal with a maximum S/N ratio. By considering the dependence of each term on  $\phi$ , the optimized dispersion signal is obtained when  $|\Delta\theta|, |\Delta\alpha L| \ll |\phi_o| \ll 1$ .

As an alternative way, one can use a balanced polarimeter consisting of a PBS and a balanced detector, as shown in Fig. 1, in order to measure only the rotation of the polarization axis. Here the half-wave plate rotates the polarization axis of the probe beam by  $45^\circ$ , and the reflected and transmitted intensities from the PBS correspond to the case of  $\phi = \pm 45^\circ$  in Eq. (1). Since the second term in Eq. (1) is maximum (minimum) when  $\phi = +45^\circ$  ( $-45^\circ$ ) and the signs of the first and third terms are the same for  $\phi = \pm 45^\circ$ , we can cancel out the background and second-order terms by using the balanced detector, which measures the difference as

$$\begin{aligned} \Delta I_t &= I_t(45^\circ) - I_t(-45^\circ) \\ &= 2I_0 \exp(-\bar{\alpha}L) \Delta\theta. \end{aligned} \quad (2)$$

For an optically thin sample ( $\bar{\alpha}L \ll 1$ ), the leading term of Eq. (2) is  $2I_0 \Delta\theta$ , showing a complete dispersion signal with no background. In addition, its magnitude is enhanced by a factor of  $2/\sin 2\phi_o \sim 1/\phi_o$ , compared with the conventional scheme with the optimized angle  $|\phi_o| \ll 1$ . Thus this DLIB spec-

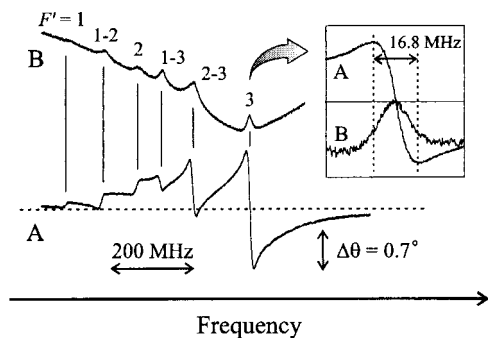


Fig. 2. The Doppler-free spectra of  $5S_{1/2} F = 2 \rightarrow 5P_{3/2} F'$  transition of  $^{87}\text{Rb}$  atoms acquired by (A) polarization spectroscopy and (B) saturated-absorption spectroscopy. The dashed line indicates a ground level of the detector. An enlarged signal of the  $F = 2 \rightarrow F' = 3$  transition is shown in the inset to indicate the relative position of the two traces.

trum is well suited for the frequency-discrimination signal.

### 3. Experiments and Results

#### A. Polarization Spectroscopy

The experimental arrangement is shown in Fig. 1. The laser source was a grating-feedback external-cavity laser diode (ECLD) in a Littrow configuration. Its wavelength was 780 nm, and a laser beam of  $\sim 0.2$  mW was sampled for the polarization spectroscopy. The pump and probe beams were led into a 5-cm-long Rb vapor cell from opposite directions with a small angle of  $\sim 3^\circ$ . The total power (intensity) was 0.1 mW ( $0.8 \text{ mW/cm}^2$ ) and  $25 \mu\text{W}$  ( $0.3 \text{ mW/cm}^2$ ) for the pump and probe beams, respectively. In the actual experiment, the half-wave plate was carefully adjusted such that the output of the balanced detector was zero in an off-resonant condition. The Rb cell was kept at room temperature and enclosed by a  $\mu$ -metal magnetic shield by which the residual magnetic field was reduced to less than 0.01 G. This shield is essential for obtaining large and stable signals, because a stray magnetic field is disruptive in two ways in the experiment. First, a transverse magnetic field orthogonal to the optical axis accelerates the decay between the magnetic sublevels, owing to spin precession. Second, the longitudinal field induces a magneto-optical effect owing to the resonance frequency difference of the  $\sigma^\pm$  components.<sup>5,6,15,16</sup> This results in the additional rotation of the polarization axis, which shifts the zero-signal level of a DLIB spectrum. Therefore the field fluctuation makes the locking point unstable. These effects will be discussed later.

With this setup, we performed the polarization spectroscopy of the  $F = 2 \rightarrow F' = 1, 2, \text{ and } 3$  transitions of  $^{87}\text{Rb}$  atoms, as shown in trace A of Fig. 2. The saturated-absorption spectrum recorded with the same sweep range is also shown in trace B as a reference. Six resonances, including three crossover transitions, can be clearly identified in trace A; the

DLIB signal of each transition has a dispersion shape as expected in Eq. (2)<sup>17</sup> with a highly improved S/N ratio over the conventional crossed polarizer scheme reported in Ref. 10. In particular, the dispersion signal for the  $F = 2 \rightarrow F' = 3$  transition has the largest amplitude and less offset, and is ideal for frequency stabilization. The peak-to-peak linewidth of this transition is 16.8 MHz, which is somewhat broader than the resolution limit of the saturated spectroscopy determined by twice a natural linewidth  $\sim 2\Gamma = 12$  MHz, owing to the power broadening; the total saturation parameter  $s$  of the pump and probe beams was 0.7, which produced the net linewidth of  $2(1 + s)^{1/2}\Gamma = 15.6$  MHz.

We observed no significant difference between the zero-crossing point of the dispersion signal for the  $F = 2 \rightarrow F' = 3$  transition and the center of the saturated-absorption spectrum, as shown in the inset of Fig. 2, whereas the other transitions had large offsets, making the line center unclear. Because this offset is due to the overlap of the long tails of the neighboring dispersion profiles,<sup>9</sup> a larger energy-level spacing and a smaller magnitude of the neighboring transitions result in a smaller offset. Here we estimate this offset induced by the crossover transition of  $F' = 2$  and 3 to the center of  $F = 2 \rightarrow F' = 3$  transition. The off-resonant rotation of the polarization axis is approximately given by  $\Delta\theta_{\text{max}}\Gamma_e/2\delta$ , where  $\Delta\theta_{\text{max}}$  is the peak-to-peak rotation angle of polarization,  $\Gamma_e$  is the peak-to-peak linewidth of the dispersion signal, and  $\delta$  is the frequency difference between the two transitions. Substituting the parameters of the present case,  $\Delta\theta_{\text{max}} = 1.0^\circ$ ,  $\Gamma_e = 16.8$  MHz, and  $\delta = 134$  MHz, into this formula, we obtain the rotation angle of approximately  $0.06^\circ$ , which corresponds to the frequency offset of only 500 kHz.

The quantitative calculation of the relative magnitude of the polarization spectrum requires the optical pumping theory in systems of up to four levels with various combinations of the Zeeman sublevels,<sup>18</sup> but this would be laborious and is not the aim of this paper. Therefore we will indicate only the qualitative interpretation of the spectrum in a complete pumping limit. Let us consider the optical pumping by the  $\sigma^+$ -polarized pump beam. All of the atoms are assumed to be transferred into the  $|F, m_F\rangle = |2, 2\rangle$  sublevel,<sup>19</sup> as shown in Fig. 3. The signal magnitude is then proportional to the difference between the relative transition strengths,  $S_+$  and  $S_-$  of  $\sigma^+$  and  $\sigma^-$  transitions from this sublevel.<sup>11,18</sup> The magnitude of  $S_+$  and  $S_-$  are also shown in Fig. 3.

There are two reasons for which the signal of the  $F = 2 \rightarrow F' = 3$  transition was largest. First,  $S_+ - S_-$  is  $30 - 2 = +28$  [Fig. 3(a)], which is larger than that of  $F = 2 \rightarrow F' = 1$  and 2 transitions from the  $|2, 2\rangle$  sublevel. Second, unlike the  $F = 2 \rightarrow F' = 1$  and 2 transitions, the  $F = 2 \rightarrow F' = 3$  transition is closed owing to the electric dipole selection rules and is free from hyperfine pumping, which depletes the number of atoms in the  $F = 2$  state and diminishes the DLIB signal.

The polarity of the dispersion signal can also be

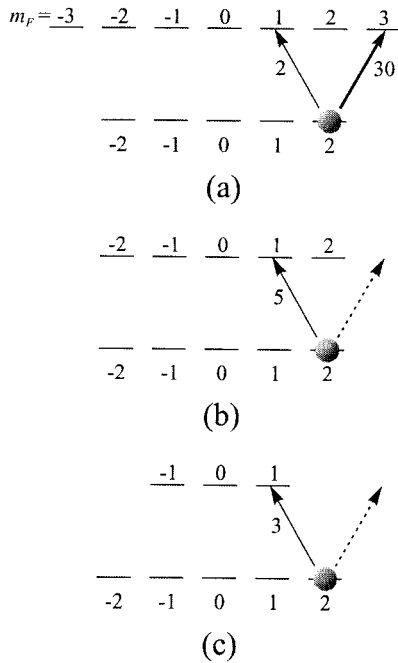


Fig. 3. The ground-state population pumped by the  $\sigma^+$ -polarized light for  $F = 2$  to (a)  $F' = 3$ , (b)  $F' = 2$ , and (c)  $F' = 1$  transitions of  $^{87}\text{Rb}$  atoms. The arrows and nearby numbers indicate the  $\sigma^\pm$  transitions and their relative strength, respectively.

understood by this simple picture. For the  $F = 2 \rightarrow F' = 2$  transition, as shown in Fig. 3(b), the  $|2, 2\rangle$  sublevel has no electronic excited state for  $\sigma^+$  transition. Therefore only the  $\sigma^-$  component of the probe beam interacts with the atoms. At this transition,  $S_+ - S_-$  is  $-5$  (negative), so the dispersion shape of this transition is inverted compared with the  $F = 2 \rightarrow F' = 3$  transition. This signal inversion also occurs for  $F = 2 \rightarrow F' = 1$  transition owing to the same reason ( $S_+ - S_- = -3$ ). Discussion of the magnitudes and polarities of the crossover transitions are also possible when the contributions from the two concerned transitions are averaged.

#### B. Laser Diode-Frequency Stabilization

As already mentioned, the advantage of the present method is not only the simplicity of the experimental system but also the achievable bandwidth of the feedback. In the ordinary laboratory environment, a major factor of the laser-diode frequency fluctuation is acoustic noise up to 10 kHz and  $1/f$  noise up to 100 kHz at most.<sup>13,20</sup> These noises are still narrower than the atomic response limit  $\sim \Gamma$ . Therefore these noises can be suppressed with a simple electronic servo with 100-kHz bandwidth.

In the experiment, we demonstrated frequency stabilization to the  $F = 2 \rightarrow F' = 3$  transition. We applied the output signal from the balanced polarimeter to the  $P$ - $I$  servo controller, and then fed the controller output back to the driving voltage of the piezoelectric transducer attached to the grating of the ECLD and the injection current of the laser diode. The bandwidth of the detector was 250 kHz, and that

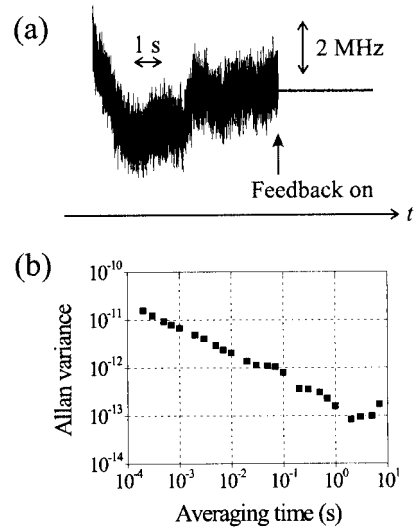


Fig. 4. (a) Monitor trace of the output of the balanced polarimeter with and without feedback. The laser frequency was initially tuned around the center of the  $F = 2 \rightarrow F' = 3$  transition. (b) Allan variance of the output signal of the polarimeter when the feedback is active.

of the overall feedback loop was 10 Hz for the piezoelectric transducer and 130 kHz for the injection current. Figure 4(a) shows the monitor trace of the detector signal when the laser frequency was tuned to around the center of the transition. From its power spectrum, we identified the dominant frequency noise as the acoustic and  $1/f$  noise up to 40 kHz. The laser linewidth within the detector's bandwidth ( $\sim 250$  kHz) was calculated from the rms fluctuation of this signal and the central slope of the dispersion profile.<sup>3</sup> With the feedback off, it was  $\sim 1.7$  MHz. When the feedback was turned on, the frequency fluctuations were efficiently suppressed from dc to  $\sim 100$  kHz, and the resultant linewidth was reduced to about 65 kHz. Using this system, we continuously stabilized the laser frequency for more than 1 day.

#### 4. Discussion

The residual fluctuation of the stabilized signal was still several times larger than the background noise floor (the noise of the electronic circuits), and therefore we evaluated the stability of the lock system by the Allan variance of the error signal, as shown in Fig. 4(b). Although this diagnosis does not always correspond to the frequency fluctuation directly, it is simple and useful.<sup>3,4</sup> When the averaging time was 2 s, the best stability was obtained as  $8 \times 10^{-14}$ , which corresponds to a fluctuation of 30 Hz. For a longer term ( $>1$  hour), however, drift of the zero-signal level, which is caused mainly by an additional polarization rotation independent of the atomic birefringence, becomes a major problem. We observed that the spectrum showed a long-term fluctuation of the entire offset, with the shapes of each transition almost unchanged. The corresponding drift of the locking point was  $\sim 1$  MHz/h. However, we could

improve it to less than 70 kHz/h by enclosing the apparatus in an acrylic box to prevent the ambient-temperature fluctuation. Therefore we attributed this drift to a temperature-dependent birefringence of the Rb-cell windows and optical elements.<sup>5</sup>

We also checked the influence of magnetic fields on the signal drift. We first applied a longitudinal magnetic field to the Rb cell inside the magnetic shield. As the field increased, the Doppler-broadened structure grew linearly around the DLIB signal. It then raised or lowered the zero-signal level, depending on the direction of the magnetic field, whereas the intensity of the DLIB signal was almost unchanged. This can be regarded as the magneto-optical rotation (MOR) or the Macaluso-Corbino effect,<sup>15,16</sup> in which  $\Delta n$  at an absorption line center no longer vanishes, owing to the Zeeman shift.<sup>6</sup> Because only the probe beam is involved in this process, the resultant MOR is Doppler broadened. This was verified by the fact that the DLIB spectrum completely vanished but the Doppler structure still remained when we blocked the pump beam before the Rb cell. The measured MOR was  $0.03^\circ/(\text{G cm})$  at the peak or the bottom of the Doppler structure, which corresponded to a frequency shift of approximately 0.7 MHz/G in our apparatus.

A transverse magnetic field in the Rb cell can destroy the spin polarization and decrease the signal magnitude. In fact, we observed that the DLIB spectra diminished by a factor of five, accompanied with a small change in the zero-signal level when we opened the magnetic shield. We interpreted this as follows. The transverse component of the external magnetic field degrades the DLIB signal, whereas the longitudinal component induces the MOR. Therefore we conclude that eliminating stray magnetic fields is an important and critical factor for obtaining high-contrast, stable DLIB spectra.

## 5. Conclusion

We have demonstrated simple, low-cost, stable, and high-speed frequency stabilization of an external-cavity laser diode by using Doppler-free light-induced birefringence in a Rb vapor. Polarization spectroscopy with the balanced polarimeter allows us to cancel out the background amplitude noise and second-order birefringence and dichroism and to enhance the signal magnitude for first-order birefringence. The obtained signal had a pure dispersion shape and contained wideband information about the laser frequency fluctuations. Use of the obtained signal as a frequency-discrimination error signal ensures robust, high-speed frequency stabilization that suppresses the acoustic and  $1/f$  noise up to several tens of kilohertz in a typical laboratory environment.

This work was supported by the Grants in Aid for Scientific Research from the Ministry of Education, Science, Sports, and Culture. After submission of this paper, we found similar research.<sup>21</sup> A preliminary report of the present locking scheme appeared in Ref. 22.

## References and Notes

1. G. C. Bjorklund, "Frequency-modulation spectroscopy: a new method for measuring weak absorptions and dispersions," *Opt. Lett.* **5**, 15–17 (1980).
2. A. Yariv, *Quantum Electronics*, 3rd ed. (Wiley, New York, 1989), chap. 14.
3. U. Tanaka and T. Yabuzaki, "Frequency stabilization of diode laser using external cavity and Doppler-free atomic spectra," *Jpn. J. Appl. Phys.* **33**, 1614–1622 (1994).
4. T. Mitsui, K. Yamashita, and K. Sakurai, "Diode laser-frequency stabilization by use of frequency modulation by a vibrating mirror," *Appl. Opt.* **36**, 5494–5498 (1997).
5. K. L. Corwin, Z.-T. Lu, C. F. Hand, R. J. Epstein, and C. E. Wieman, "Frequency-stabilized diode laser with the Zeeman shift in an atomic vapor," *Appl. Opt.* **37**, 3295–3298 (1998).
6. V. V. Yashchuk, D. Budker, and J. R. Davis, "Laser frequency stabilization using linear magneto-optics," *Rev. Sci. Instrum.* **71**, 341–346 (2000).
7. C. I. Sukenik, H. C. Busch, and M. Shiddiq, "Modulation-free laser frequency stabilization and detuning," *Opt. Commun.* **203**, 133–137 (2002).
8. C. Wieman and T. W. Hänsch, "Doppler-free laser polarization spectroscopy," *Phys. Rev. Lett.* **36**, 1170–1173 (1976).
9. J. B. Kim, H. J. Kong, and S. S. Lee, "Dye laser frequency locking to the hyperfine structure ( $3S_{1/2}$ ,  $F = 2 - 3P_{1/2}$ ,  $F = 2$ ) of sodium  $D_1$  line by using polarization spectroscopy," *Appl. Phys. Lett.* **52**, 417–419 (1988).
10. G. P. T. Lancaster, R. S. Conroy, M. A. Clifford, J. Arlt, and K. Dholakia, "A polarisation spectrometer locked diode laser for trapping cold atoms," *Opt. Commun.* **170**, 79–84 (1999).
11. W. Demtröder, *Laser Spectroscopy* (Springer, Berlin, 1981), chap. 7.
12. C. Delsart and J.-C. Keller, "Laser-induced dichroism and birefringence in two- and three-level systems of neon," *J. Appl. Phys.* **49**, 3662–3666 (1978).
13. C. Petermann, *Laser Diode Modulation and Noise* (Kluwer Academic, Boston, 1988), chap. 7.
14. The numerator  $\Delta n k_0 L$  represents the relative phase difference between the two circularly polarized components.
15. D. Budker, D. J. Orlando, and V. Yashchuk, "Nonlinear laser spectroscopy and magneto-optics," *Am. J. Phys.* **67**, 584–592 (1999).
16. D. Budker, W. Gawlik, D. F. Kimball, S. M. Rochester, V. V. Yashchuk, and A. Weis, "Resonant nonlinear magneto-optical effects in atoms," *Rev. Mod. Phys.* **74**, 1153–1201 (2002).
17. Although the optical density of the saturated absorption  $\bar{\alpha}L$  was  $\sim 0.3$  in the actual experiment, Eq. (2) still represents an almost-pure dispersion signal.
18. S. Nakayama, "Polarization spectroscopy of Rb and Cs," *Opt. Commun.* **50**, 19–25 (1984).
19. For the  $F = 2 \rightarrow F' = 1$  transition, the  $|2, 1\rangle$  sublevel is also the pumped state of the  $\sigma^+$ -polarized light. However, the qualitative discussion in the context is still valid when the atoms are populated in both  $|2, 2\rangle$  and  $|2, 1\rangle$  sublevels.
20. L. D. Turner, K. P. Weber, C. J. Hawthorn, and R. E. Scholten, "Frequency noise characterisation of narrow linewidth diode laser," *Opt. Commun.* **201**, 391–397 (2002).
21. C. P. Pearman, C. S. Adams, S. G. Fox, P. F. Griffin, D. A. Smith, and I. G. Hughes, "Polarization spectroscopy of a closed transition: applications to laser frequency locking," *J. Phys. B* **35**, 5141–5151 (2002).
22. Y. Sasaki, K. Ito, Y. Yoshikawa, K. Kondo, Y. Torii, T. Kuwamoto, and T. Hirano, "Department of a narrow band high power laser system using a broad-area diode laser," in *Meeting Abstracts of the Physical Society of Japan* (Physical Society of Japan, Tokyo, 2001), Vol. 56, p. 93.